Phase recovery by using optical fiber dispersion

C. Cuadrado-Laborde,[1,2,3,*] A. Carrascosa,[1] P. Pérez-Millán,[1] A. Díez,[1] J. L. Cruz,[1] and M. V. Andres[1]

[1]*Departamento de Física Aplicada, ICMUV, Universidad de Valencia, Dr. Moliner 50, Burjassot E-46100, Spain*

[2]*Instituto de Fisica Rosario (CONICET-UNR), Ocampo y Esmeralda, S2000EZP, Rosario, Argentina*

[3]*Facultad de Ciencias Exactas e Ingeniería, Universidad Católica de La Plata, Buenos Aires, Argentina*

**Corresponding author: Christian.Cuadrado@uv.es*

Received August 15, 2013; revised December 9, 2013; accepted December 21, 2013;
posted December 23, 2013 (Doc. ID 195877); published January 28, 2014

We propose a simple and fast procedure to retrieve the phase profile of arbitrary light pulses. It combines a first experimental stage, followed by a one-step numerical stage. To this end, it is necessary to perform a Fresnel transform, which is obtained just by propagating the light pulses through an optical fiber. We experimentally test this proposal recovering the phase profile in the light pulses provided by a passively mode-locked laser. The proposal is then compared with a temporal variation of the Gerchberg–Saxton recursive algorithm, which is specially modified for this purpose. © 2014 Optical Society of America

OCIS codes: (120.5050) Phase measurement; (350.5030) Phase.
http://dx.doi.org/10.1364/OL.39.000598

In space optics, there are several successful recursive algorithms for phase reconstruction from the intensity of the signal and its Fourier or Fresnel transform (FT and FrT, respectively) [1,2]. Despite this, the development of nonrecursive procedures remains an attractive field of research. Teague developed a nonrecursive approach for phase retrieval [3], which was further developed by others [4,5]. It was demonstrated that the longitudinal derivative of the Fresnel spectrum is proportional to the transversal derivative of the product of the instantaneous intensity and frequency of the signal. This was known as the transport-of-intensity equation (TIE); a similar technique also holds for the fractional FT [6,7]. Later, Dorrer translated to the temporal domain the TIE to determine the nonlinear coefficients of a highly nonlinear fiber [8].

The phase recovery, or its first temporal derivative, i.e., the instantaneous angular frequency, is an important characteristic of nonstationary signals. Its monitoring is of great importance in fiber-optic communication systems today. Recently, it was shown that a spectrally shifted differentiator can be used to retrieve the phase profile of a given temporal optical waveform [9]. However, the operation is performed by using short or long period fiber gratings, which have fixed operation wavelengths, and restrictive operation bandwidths. In [10,11], a phase-recovery technique was proposed from temporal intensity measurements at the input and output of a linear optical filter. However, precise knowledge of the filter's impulse response is necessary in amplitude and phase, together with the additional restriction in the later to be limited to a maximum variation range of π rad through the whole operation bandwidth.

In this work, we propose a simple phase-recovery technique that combines a first experimental stage followed by a direct numerical stage. In the experimental stage, it is necessary to acquire two temporal intensity profiles at the input and output of a linear dispersive device. In the numerical stage, a single equation is applied to retrieve the phase profile in just one step. This proposal could be considered within the framework of the use of dispersive elements to characterize optical signals by using oscilloscope measurements. As an example, dispersive FT has emerged as a successful technique enabling fast measurements in optical sensing, spectroscopy, and imaging (see [12] and references therein). As a proof-of-concept, the proposal is experimentally tested, retrieving the temporal phase profile of a passively mode-locked laser. Then the results are compared with a time-domain variation of the Gerchberg–Saxton algorithm (GSA) [1,13].

The FrT of a given 1D complex signal $f(t) = |f(t)|\exp[j\varphi(t)]$ can be expressed by

$$f_\alpha(t) = (2\ \pi \mathrm{j}\alpha)^{-1/2}\int_{-\infty}^{\infty} \mathrm{d}\tau f(\tau)\exp\left[-j\frac{1}{2}(t-\tau)^2/\alpha\right], \quad (1)$$

where $f_\alpha(t)$ is the FrT signal, and α is the FrT parameter. By using Eq. (1), and after some algebraic manipulations, it is possible to demonstrate the following equality [7]:

$$\varphi(t) = \varphi_0 + \int_{-\infty}^{t} \mathrm{d}t'\left[\frac{1}{|f(t')|^2}\int_{-\infty}^{\infty}\mathrm{d}\tau\left.\frac{\partial|f_\alpha(\tau)|^2}{\partial\alpha}\right|_{\alpha=0} H(t'-\tau)\right], \quad (2)$$

where φ_0 is an arbitrary phase constant and $H(\cdot)$ is the Heaviside step function. The expression between the square brackets in Eq. (2) is known as the temporal TIE. It links the variations of the temporal intensity that are due to dispersive propagation to the temporal intensity and phase.

Now let us focus on the propagation of a given optical temporal signal by a dispersive medium such as an optical fiber of length L. Dispersive media can be modeled as linear time invariant systems by means of a transfer function. Let this transfer function $S(\omega)$ have flat amplitude and quadratic phase response (i.e., linear group delay) over a certain operative spectral bandwidth:

$$S(\omega) = \exp\left[j\frac{1}{2}\Phi_{20}\omega^2\right] \overset{\mathrm{FT}^{-1}}{\rightarrow} s(t) \propto \exp[-jt^2/2\Phi_{20}], \quad (3)$$

where ω is the baseband angular frequency, $s(t)$ is the impulse response, which was obtained by inverse FT of $S(\omega)$, and Φ_{20} is the first-order dispersion coefficient;

being $\Phi_{20} = L\beta_{20}$, where β_{20} is the second-order derivative of the propagation constant. Additionally, and only for simplicity, the average time delay has been ignored. The propagation of a single pulse for a linear dispersive regime can be expressed by convolving $f(t)$ with $s(t)$. Therefore, except by a multiplicative constant, we recognize in the right-hand side of Eq. (3) the FrT kernel of Eq. (1), with FrT parameter $\alpha = \Phi_{20}$. Thus we can perform the required FrT just by propagating the input optical pulse by a dispersive device, such as an optical fiber, or by reflection in a linearly chirped fiber Bragg grating. Regarding the derivative of the signal intensity with respect to the FrT parameter, see Eq. (2), we propose its replacement by a finite difference as follows:

$$\partial|f_\alpha(t)|^2/\partial\alpha\big|_{\alpha=0} \approx [|f_\alpha(t)|^2 - |f(t)|^2]/\alpha\big|_{\alpha\to 0}. \tag{4}$$

From now on we will refer to the numerator of the right-hand side of Eq. (4) as the temporal profile difference (TPD). The approximation given by Eq. (4) improves as the dispersion length L is reduced, since $\alpha = \Phi_{20} = L\beta_{20}$. However, in practice, the presence of noise imposes a lower limit for the reduction of the dispersion length, being necessary for a satisfactory phase recovery that the TPD be higher than the noise level. As a rule of thumb, the lower the signal-to-noise ratio (SNR) is, the higher the necessary dispersion length. However, the dispersion length cannot be increased indefinitely because the validity of Eq. (2) is restricted to the near-field regime, where the following inequality holds $\Delta t^2/2\pi\Phi_{20} \gg 1$, where Δt is the time width of the input signal. In this way, by replacing $\Phi_{20} = L\beta_{20}$ and rearranging, we find the higher limit for the dispersion length:

$$L \ll \Delta t^2/2\pi\beta_{20}. \tag{5}$$

If inequality of Eq. (5) is not fulfilled, we would be in the far-field Fraunhofer regime, where the transmitted signal envelope is, within a phase factor, proportional to the FT of the input signal envelope [14]. Generally, a trade-off between precision and quality of the TPD will be necessary to find the optimum dispersion length. Interestingly, when an optical fiber is used as a dispersive medium, this does not represent a major issue. Finally, we summarize in Table 1 the proposed procedure for the phase profile retrieving.

We will compare the results obtained with a time-domain analog of the GSA. The GSA was originally developed to retrieve the phase of a spatial image based on intensity recordings in the image and diffraction planes [1]. The method depends on there being a FT relation between the waves in these two planes. However, an adaptation of this concept is suitable for the present problem, replacing the FT by a FrT [13], relaxing in this way the use of high dispersion values. The procedure for reconstruction requires the measurement of the envelopes of the original and FrT signals, $|f(t)|$ and $|f_\alpha(t)|$, respectively; both are obtained by taking the square root of the measured temporal intensity profiles (a previous numerical area normalization and time alignment is also necessary). The proposed algorithm is illustrated schematically in Fig. 1, which should be followed clockwise. To begin the procedure (upper-left corner), an initial guess for $\varphi(t)$ is required. The phase guess and measured magnitude are combined and numerically FT. Once in the frequency domain, the quadratic phase due to dispersion $S(\omega)$ is applied [see Eq. (3)], and the waveform is transformed back to time. At this point, only the calculated phase $\theta(t)$ is retained; the calculated magnitude is replaced by the measurement $|f_\alpha(t)|$. The calculated phase and measured magnitude are combined and numerically FT. Once in the frequency domain, the quadratic phase due to dispersion is removed by using $S^{-1}(\omega)$, and the waveform is transformed back to time. The cycle is then completed by using the measurement again at the beginning, but retaining the calculated phase. The GSA is a recursive process, and it should be repeated at the user's discretion.

Table 1. Procedure for Phase Recovery by FrT Technique

Stage	Description
Experimental	0. The dispersion of the optical fiber used to perform the FrT should be known; otherwise must be measured
	1. Data acquisition of the temporal intensity profiles of the optical pulse whose phase will be retrieved and of its FrT
Numerical	2. Area normalization and time alignment of both temporal intensity profiles
	3. The phase is recovered using Eqs. (2) and (4)

When the input optical pulse is short enough that it cannot be measured by an oscilloscope—let us denote by $f_0(t)$—it becomes necessary to pre-stretch the pulse by using another dispersive media, with transfer function $S_0(\omega)$, until it can be detected. This detected pre-stretched pulse plays the role of $|f(t)|^2$, which should be further dispersed and detected, being this signal $|f_\alpha(t)|^2$. The FrT technique, or GSA, is then applied as described above to recover the phase of the pre-stretched pulse $\varphi(t)$. Finally, the input optical pulse can be obtained, in both modulus and phase, through $f_0(t) = \mathrm{FT}^{-1}\{\mathrm{FT}\{|f(t)|\exp[j\varphi(t)]\}/S_0(\omega)\}$.

As a proof-of-concept, we demonstrate the feasibility of these proposals by experimentally retrieving the phase in the light pulses provided by an all-fiber passively mode-locked laser. Since these pulses are long enough, in this case it is not necessary to apply the pre-stretching technique described above. Thus different FrTs were obtained by using different lengths of a standard optical fiber as the dispersive device. The light pulses provided by the mode-locked laser were split by a 50/50 coupler (see Fig. 2). At one of the output ports, we detected the light pulses of the mode-locked laser with a > 63 GHz

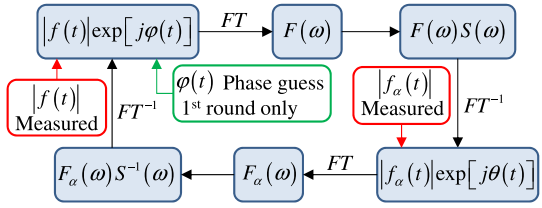

Fig. 1. GSA for temporal phase retrieval at the input by FrT.

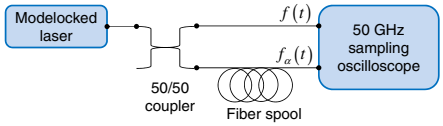

Fig. 2. Experimental setup.

sampling oscilloscope provided with a fast built-in photodetector (53 GHz); this signal is $|f(t)|^2$ in Eq. (4). We also simultaneously propagated the light pulses provided by the mode-locked laser by an optical fiber of a given length in order to obtain the FrT; this signal is also registered by the oscilloscope, being $|f_\alpha(t)|^2$ in Eq. (4). If the dispersion of the optical fiber is known, the experimental stage finishes with the acquisition of both temporal profiles.

The procedure to retrieve the phase profile continues numerically by using as working files $|f_\alpha(t)|^2$ and $|f(t)|^2$ (see Table 1). An important digression is in order here; the energy of the two signals should be equal, since the FrT—as a member of the unitary canonical transforms—preserves the signal's energy. Further, both signals must be synchronized as well, since time delay effects have been ignored in the derivation of Eq. (2). Fortunately, it is not necessary to perform these tasks experimentally, since both operations can be more easily performed in the numerical stage. The power losses are numerically fixed, equalizing both pulse energies, i.e., areas, by multiplying one of both profiles by a numerical constant. The time delay, on the other hand, is numerically removed by temporally matching the intensity maxima of both profiles. The error that these numerical operations could introduce in the measured phase has not been evaluated yet, although, by repeating the measurements with different lengths of fibers, we are reducing the possibilities of having a systematic error from just one measurement.

The passively mode-locked ytterbium fiber laser provided light pulses at an emission wavelength $\lambda_0 =$ 1038 nm with a repetition rate of 23.15 MHz, which can be satisfactory adjusted with a sech profile $|f(t)| =$ $\mathrm{sech}(t/T_0)$, where $T_0 = 12$ ps, i.e., a FWHM of 20 ps. The dispersion line was made with a low numerical aperture optical fiber (SM980 by Fibercore). We measured by the interferometric technique the first-order dispersion at λ_0 of this optical fiber resulting in $D = -44$ ps/nm × km, and by using $\beta_{20} = -\lambda_0^2 D/2\pi c$, with c the speed of light in vacuum, results $\beta_{20} = 25.1$ ps^2/km. Therefore, by using Eq. (5), with $\Delta t = 4T_0$, results in $L \ll 14$ km. Taking into account this higher limit for the dispersion length, three different fiber lengths were used $L = 315$, 214, and 101 m. Thus, for each specific fiber length, Φ_{20} results in 7.94 ps^2 (315 m), 5.4 ps^2 (214 m), and 2.54 ps^2 (101 m). The nonlinear length L_{NL} was obtained from $L_{\mathrm{NL}} = (\gamma P_0)^{-1} =$ 3.8 km, where $P_0 = 51$ mW is the peak power of the optical pulses (derived using a measured average power of 23.54 μW) and the nonlinear parameter $\gamma \approx$ 0.0052 W^{-1}/m (derived using a mode field diameter of 6.2 μm and a nonlinear parameter $n_2 = 2.6\times$ 10^{-20} m^2/W). Since the selected dispersion lengths are well below the nonlinear length, from now on we can safely ignore the influence of nonlinear effects in our measurements. Figure 3(a) shows the experimentally measured light pulses to the input of the dispersive

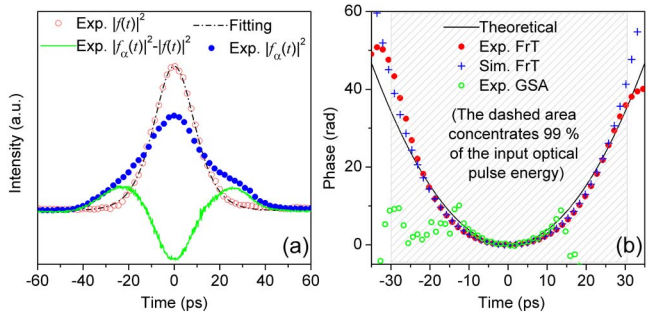

Fig. 3. (a) Measured temporal profiles at the input (plus the corresponding fitting) and output of a fiber length of 315 m, the TPD is also shown. (b) Phase recovered by the proposed FrT technique, experimentally and numerically (Exp. FrT and Sim. FrT, respectively), as compared with the phase experimentally recovered by the modified GSA, a theoretical parabolic phase profile with $C = -11$ is also shown.

device (together with its corresponding fitting), the experimentally measured FrT pulse—with parameter $\alpha =$ $\Phi_{20} = 7.94$ ps^2 (315 m)—and the TPD. The temporal phase profile was directly recovered from the raw data applying Eqs. (2) and (4), being unnecessary to smooth previously the data set [see Exp. FrT curve in Fig. 3(b)]. The instantaneous angular frequency—obtained by the first-order temporal derivative of the temporal phase profile, not shown—increases monotonously from the leading to the trailing edge of the pulse; this is currently known as an up-chirp.

We also fitted a phase profile for the light pulses of the mode-locked laser, using as $|f(t)|^2$, the sech profile obtained by fitting the light pulses provided by the mode-locked laser, shown in Fig. 3(a). However, since $f(t)$ is evidently chirped, we simulate this by adding to the sech profile a linearly chirped term in the following way $f(t) = \mathrm{sech}(t/T_0) \times \exp(-jCt^2/2T_0^2)$, where C is the chirp-dimensionless parameter. On the other hand, $|f_\alpha(t)|^2$ was obtained by simulating the propagation of this linearly chirped sech profile by a dispersive media characterized by Eq. (3), with $\alpha = \Phi_{20} = 7.94$ ps^2. From these two simulated signals, we calculated a simulated phase profile by using Eqs. (2) and (4). To this end, we tried different chirp parameters to fit the simulated phase profile to the experimental data. Best results were obtained for a chirp parameter $C = -11$, the simulated phase profile is also shown in Fig. 3(b) (Sim. FrT). The degree of resemblance between both experimental and simulated phase profiles is remarkable, indicating that the light pulses provided by the mode-locked laser are linearly up-chirped. We emphasize that we should focus our attention to the region where the pulse energy is localized. The theoretical parabolic phase profile with $C = -11$ is also shown. Finally, we also shown in Fig. 3(b) the phase recovered by our modification to the GSA, after 170 roundtrips. They match with reasonable accuracy, although it is evident that the reconstructed phase obtained by the present method is better than that obtained by the GSA. It should be mentioned also that the GSA depends on an educated guess for the phase, whereas here it is not necessary. Finally, it is notable to emphasize the different computation times necessary for the phase recovery by using the FrT

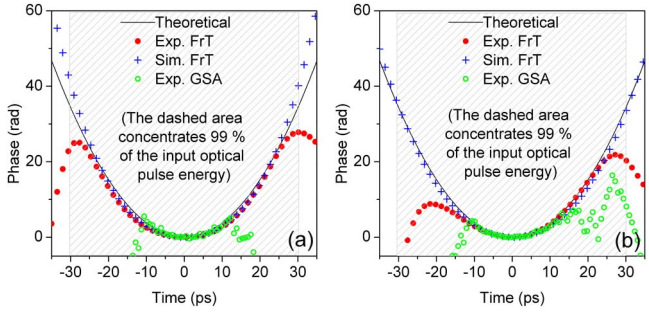

Fig. 4. Same as in Fig. 3(b), but for a fiber length of 214 m (a) and 101 m (b).

technique and the GSA. In the former, it is necessary just one single mathematical step; as a result, the phase is recovered instantly, whereas in the GSA two FT and two anti-FT are performed for every roundtrip. As a consequence, the computation time required for the GSA is considerably longer. Related with this, it is worth mentioning that the technique proposed in [10,11] is iterative, i.e., the phase is recovered point-by-point through the whole sample data.

Since the TPD shown in Fig. 3(a) is well above the noise level, there is margin for a further reduction in the fiber length in order to study the influence of the approximation introduced by Eq. (4). Thus we experimentally retrieve the phase by using $\alpha = \Phi_{20} = 5.4$ ps^2 (214 m) and $\alpha = \Phi_{20} = 2.54$ ps^2 (101 m). By applying Eq. (2) via Eq. (4) once again, we experimentally retrieve the phase profiles for these new dispersion lengths, which are shown in Figs. 4(a) and 4(b), for 214 and 101 m, respectively. The simulated phase profiles are also shown in both cases; again the degree of resemblance between both experimental and simulated phase profiles remains satisfactory. Finally, the phase recovered by our modification to the GSA is also shown in Figs. 4(a) and 4(b), matching with reasonably accuracy. The phases finally recovered are essentially the same independently of the fiber length used, although it is clear that for the shorter fiber length (101 m) the TPD is the worst determined. This is something to be expected, since for short propagation lengths output and input pulses become essentially the same signal.

We also studied the robustness of the proposed technique by simulating additive and independent white noise in the input and output temporal profiles. In Fig. 5(a), we show the phase directly recovered with the unsmoothed data when the SNR = 10 dB, as compared with the theoretical phase (the pulse parameters and the dispersion length are the same as in Fig. 3). As observed, the phase can be satisfactorily recovered despite the strong presence of noise in the TPD [see the inset of Fig. 5(a)]. This robustness against intensity noise is related to the inherently low-pass behavior of the integral and the replacement of the original derivative by a finite difference [see Eqs. (2) and (4), respectively]. We conclude this work by demonstrating the applicability of the FrT technique to a more general phase profile. To this end, we simulated the phase-profile recovery of a super-Gaussian pulse defined by $f(t) = \exp[-(1/2)(1 + jC)(t/2T_0)^{2m}]$, with $m = 3$, $C = -3$, $T_0 = 12$ ps, and SNR = 20 dB. The inset in Fig. 5(b) shows the TPD (with $\alpha = \Phi_{20} = 2$ ps^2,

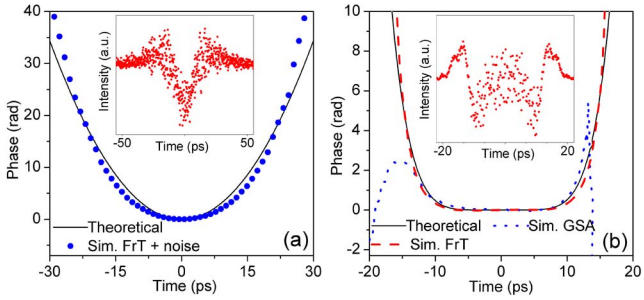

Fig. 5. (a) Simulated phase recovered by the FrT technique in the presence of noise with SNR = 20 dB, as compared with the theoretical phase. The inset shows the TPD. (b) Phase profiles numerically recovered by the FrT technique and GSA for a super-Gaussian pulse with a SNR = 20 dB; the theoretical phase profile is also shown. The inset shows the TPD.

equivalent to the dispersion of 80 m of SM980 optical fiber at 1034 nm). The retrieved temporal phase profiles of the input optical pulse by using the FrT and GSA (67 roundtrips) are shown in Fig. 5(b), together with the theoretical phase profile. The degree of resemblance between the phase profiles is satisfactory, demonstrating the applicability of this technique to retrieve arbitrary phase profiles.

In this work, we proposed and experimentally proved a simple technique to retrieve the phase profile of a temporal optical waveform. Since the measurement relies on time-domain intensity detection, the technique is limited by the bandwidth of the oscilloscopes and detectors (100 GHz in real-time electronic oscilloscopes, >500 GHz in sampling optical oscilloscopes). Among the advantages, we point out its experimental and computational simplicity and that it is intrinsically well-suited for any optical wavelength.

This work has been financially supported by the Ministerio de Ciencia e Innovación and the Generalitat Valenciana of Spain (projects TEC2008-05490, PROMETEO/2009/077, and GV/2012/121, respectively). C. Cuadrado-Laborde acknowledges the financial support from the Programa de Investigadores Invitados de la Universidad de Valencia (Spain).

References

1. R. W. Gerchberg and W. O. Saxton, Optik **35**, 237 (1972).
2. Z. Zalevsky, D. Mendlovic, and R. G. Dorsch, Opt. Lett. **21**, 842 (1996).
3. M. R. Teague, J. Opt. Soc. Am. **73**, 1434 (1983).
4. N. Streibl, Opt. Commun. **49**, 6 (1984).
5. K. Ichikawa, A. W. Lohmann, and M. Takeda, Appl. Opt. **27**, 3433 (1988).
6. T. Alieva and M. J. Bastiaans, IEEE Signal Process. Lett. **7**, 320 (2000).
7. M. J. Bastiaans and K. B. Wolf, J. Opt. Soc. Am. A **20**, 1046 (2003).
8. C. Dorrer, Opt. Lett. **30**, 3237 (2005).
9. F. Li, Y. Park, and J. Azaña, Opt. Lett. **32**, 3364 (2007).
10. M. H. Asghari and J. Azaña, Opt. Lett. **37**, 3582 (2012).
11. M. H. Asghari and B. Jalali, IEEE Photon. J. **4**, 1693 (2012).
12. K. Goda and B. Jalali, Nat. Photonics **7**, 102 (2013).
13. D. R. Solli, S. Gupta, and B. Jalali, Appl. Phys. Lett. **95**, 231108 (2009).
14. M. A. Muriel, J. Azaña, and A. Carballar, Opt. Lett. **24**, 1 (1999).